4D printed thermally activated self-healing and shape memory polycaprolactone-based polymers

Marta Invernizzi, Stefano Turri, Marinella Levi, Raffaella Suriano*

Department of Chemistry, Materials and Chemical Engineering "Giulio Natta", Politecnico di Milano, 20133, Italy

The ability to change the shape of 3D printed objects as a function of time is known as 4D printing. Shape memory polymers with their shape-changing behavior are emerging as attractive materials to produce actuators for soft robotics. They can be transformed from one shape to another by a thermo-mechanical programming process. Self-repairing capabilities are also desirable for soft actuators to enhance their durability and mimic natural tissues. The possibility to produce 4D printed polymers with shape memory effect has proven but self-healing behavior was not attained so far in 4D printed shape memory objects. The focus of the present work is to demonstrate the capability of a newly developed material and of a customized low-cost 3D printer to produce 4D printed self-repairing objects. A 4D printed shape memory polymer with thermally induced healing abilities is first presented in this work and achieved by digital light projection (DLP) technology. Shape memory and self-healing functionalities are thermally triggered and obtained respectively using polycaprolactone (PCL) chains and 2-ureido-4[1H]-pyrimidinone (UPy) units co-crosslinked in this newly prepared material. Printed PCL/UPy-based objects show a stiffness similar to PCL-based ones, a higher elongation at break and a shape memory effect better than other printed PCL samples found in literature. The printability of shape memory objects is demon-strated with the printing of an opposing thumb, capable of being moved forward to the tip of a forefinger and then backward. Shape memory functionalities are still preserved after healing, making these printed actuators suitable for the production of components for human-machine interactions and soft robotics.

Keywords: Shape memory polymers, Self-healing, 4D printing, Heat-responsive polymers, Ureido-pyrimidinone, Polycaprolactone

1. Introduction

Over the past few years, the potential of additive manufacturing, also called 3D printing [1], as a versatile technology platform for computer-assisted design (CAD) and rapid manufacturing was explored and demonstrated in a number of clear successes [2]. Several additive manufacturing technologies have been developed for processing pure polymers and polymer nanocomposites [3], such as stereolithography (SL), digital light projection (DLP), direct inkjet and extrusion-based printing as well as liquid deposition modeling (LDM) [4]. They enable less-expensive free-form fabrication of complex, customized and multi-scale 3D geometries for application in a vast range of fields, from tissue engineering scaffolds [5] to strain and skin-like sensors [6,7].

The capability to obtain four dimensional (4D) printed structures with a dynamic behavior as a function of time, where the time is the fourth dimension in the 3D space coordinates, has recently gained considerable interest [8]. 4D printing was firstly introduced by a research group of MIT and defined as the fabrication of 3D printed structures with adaptable and programmable shapes, properties or functionality as a function of time [9]. This time-dependent change in shape, property or functionality can appropriately be triggered by different types of stimuli. Gladman et al., for instance, used water to activate 4D printed water-sensitive biomimetic structures inspired by nature [10]. Other stimuli can also be utilized in 4D printing such as heat [11], pH [12], a combination of heat and water [13] as well as of heat and light [14]. The ability of 4D printed structures to self-assemble and self-repair opens new opportunities of application, such as the fabrication of minimally invasive surgery devices that can be placed in human body through a little surgical incision and then assembled at the required position for surgical operations [15]. In addition to additive manufacturing facility and stimulus, other fundamental elements of 4D printing are stimuli-responsive material, stimulus-triggered programming process and mathematical modeling, as reported by Momeni et al. [16].

One of the most crucial factors of 4D printing is the stimuli-responsive material, which receives, transmits, or processes a stimulus and respond by producing a useful effect, including an actuation mechanism or a signal that the materials are acting upon it. Over the last

Received 27 October 2017;
Received in revised form 12 February 2018;
Accepted 16 February 2018
Available online 17 February 2018

* Corresponding author.
E-mail address: raffaella.suriano@polimi.it (R. Suriano).

Published Journal Article available at https://doi.org/10.1016/j.eurpolymj.2018.02.023

two decades, the development of such smart materials has received great interest due to the potential applications in a wide range of areas, from robotics to tissue engineering and biomedical devices [17–20]. Of the possible smart materials, both self-healing polymers and shape memory polymers (SMPs) have gained ever-increasing interest [21,22].

Self-healing of polymers can be achieved by a few categories of reactions, which include covalent bonding, supramolecular chemistry, H-bonding, ionic interactions, and π–π stacking [23–25]. More recently, self-healing materials have shown great potential for producing soft actuators with enhanced durability, due to their ability to self-repair damage ranging from bulk cracks to surface scratches [26]. Moreover, the use of self-healing hydrogels as "inks" for additive manufacturing was successfully demonstrated [27].

As for SMPs, they are widely studied due to their prospective use in a variety of technological fields, including biomedical engineering [28,29], in vivo tissue regeneration [30], device microfabrication [11,31] and self-actuation [32]. This class of materials has inspired multidisciplinary researchers with the possibility to trigger shape changes in polymer systems upon an external stimulus (*e.g.* temperature, light, magnetic field, pH and moisture) [22,33], combined with biocompatibility [34,35] and ease of processing of SMPs [36]. By exploiting DLP technology, a heat-activated SMP was also 4D printed and structured, using a photocurable polycaprolactone (PCL) [31,37]. Unlike other 4D printed smart materials, SMPs require a thermo-mechanical programming process, also called constrained-thermo-mechanics, to be transformed from a permanent shape to a temporary one and vice versa [38]. The temporary shape is obtained when the material is heated above its transition temperature (T_{trans}) and deformed. The temporary shape is then fixed at $T < T_{trans}$. The permanent shape is, meanwhile, "memorized" by the material and can be recovered by heating at $T > T_{trans}$.

Drawing inspiration from multifunctional properties of natural systems such as human skin and double-helix DNA, some emerging pathways have lately combined SMP networks and self-healing materials that can respond to the same external stimulus, *i.e.* heat [39–41]. To provide intrinsic self-repairing properties to polymer materials, various strategies have been developed so far, many of which are based on either covalent bonds [42,43] or non-covalent interactions [24]. Chen et al. prepared polyurethane crosslinked networks, showing both a shape memory effect based on cyclic PCL and self-healing properties based on dynamic covalent bonds arising from a reversible Diels–Alder reaction between furan and maleimide groups [44]. As for self-healing systems based on non-covalent interactions, an example of a self-repairing polymer hydrogel was presented by Phadke et al., who exploited flexible side chains with amide and carboxylic functional groups to create hydrogen bonding across two hydrogel interfaces [45]. Many approaches developed telechelic systems functionalized with self-complementary 2-ureido-4[1*H*]-pyrimidinone (UPy) units, thus introducing multiple hydrogen bonding interactions and reversible intermolecular cross-links to be used as a trigger for a self-healing effect [40,46]. In addition to self-healing properties, UPy moieties can also improve phase component compatibility and mechanical properties of polymer blends [47].

However, in literature there are no examples that explore the potential of 4D printing for creating objects with shape memory and self-healing behavior, concurrently. We believe that this is the first work showing the 4D printing of a self-healing and shape memory polymer. The study presented here is focused on the development of a shape memory polymer that can be 4D printed to produce structures with self-repairing abilities and embedded thermally switching domains. This newly prepared material is photo-crosslinked and printed *via* DLP technology, by combining polycaprolactone dimethacrylate (PCLDMA) macro-monomers with methacrylates bearing 2-ureido-4[1*H*]-pyrimidinone motifs (UPyMA). The incorporation of UPyMA monomers provides self-healing properties to the 4D printed structures. The possibility to print actuators for soft robotics with good mechanical properties and self-healing capabilities is first shown in this work. An example of a shape-changing object, an opposing thumb with a forefinger, is presented here as a proof of concept.

2. Experimental section

All reagents were purchased from Sigma-Aldrich, Milan, except where indicated.

2.1. Methacrylation reaction

After drying PCL at 120 °C under dynamic vacuum for 2 h, the end-capping reaction was carried out by mixing PCLs with 2-isocyanatoethyl methacrylate (2-IEM, Showa Denko) at 60 °C for 2 h. A molar ratio between 2-IEM and PCL (2-IEM/PCL) of 1.9 was used. $Sn(Oct)_2$ was added in a molar ratio of 2:100 with respect to PCL. Both 2-IEM and $Sn(Oct)_2$ were pre-dissolved in the minimum quantity of $CHCl_3$. Chloroform dried under molecular sieves was also added to the system (1 ml per 1.2 g of PCL) to decrease PCL viscosity. The reaction was monitored by means of FT-IR spectroscopy, checking the disappearance of the isocyanate groups at 2275 cm^{-1}. The functionalized PCLDMA macro-monomers were precipitated in cold petroleum ether and dried overnight in a fumehood.

2.2. Ureido-pyrimidinone methacrylate monomer synthesis

6-Methyl isocytosine (MIS) (4 wt% in dimethyl sulfoxide, DMSO) was added to a round bottom flask, which was consequently sealed with a rubber septum and a condenser. After being dehydrating for 56 h under nitrogen atmosphere and in presence of molecular sieves, 50 mL of DMSO were added to the flask by a syringe and heated up to 170 °C. The temperature inside the flask was constantly monitored with a thermometer. Once the temperature of the solution reached 170 °C and the total dissolution of MIS solid powder in the solvent was obtained, the heating system was quickly removed and 2-IEM (5 wt% in DMSO, [2-IEM]:[MIS] = 1.1:1 M ratio) was immediately added to the flask with a syringe, keeping the system under vigorous stirring induced by a magnetic stirrer. Afterwards, the mixture was quickly cooled with an ice bath in order to avoid unwanted side polymerizations. Lastly, the precipitation of UPyMA monomer was induced washing the solution in a large excess of acetone, which enabled the removal of any other traces of unreacted 2-IEM monomer. The liquid suspension was then filtered, and the solid was collected and dried under vacuum at room temperature for 48 h.

2.3. Printable formulation composition and 3D printing set-up

To print self-healing shape memory polymers, we used a mixture of PCLDMA and UPyMA containing 4 wt% of 2,4,6-trimethylbenzoyl-diphenyl-phosphinoxide as photoinitiator (TPO-L, BASF, Germany) and $CHCl_3$ (60 wt% with respect to the weight of PCLDMA and UPyMA) to ensure the best diffusion of UPyMA monomers into PCLDMA. The formulation was kept at 45 °C during the printing process by a custom-made hot plate as reported in Fig. 1. After printing, the specimens underwent a post-curing of 30 min in a UV oven (DWS Systems, Italy). The printing parameters are listed in Table S1 (Supplementary Materials).

2.4. Material characterization

2.4.1. Chemical characterization

FT-IR spectroscopy analysis was carried out by means of a Nicolet 760-FTIR spectrometer in transmission mode at room temperature in air on methacrylated PCL films applied onto NaCl disks. 32 scans with a resolution of 2 cm^{-1} were performed.

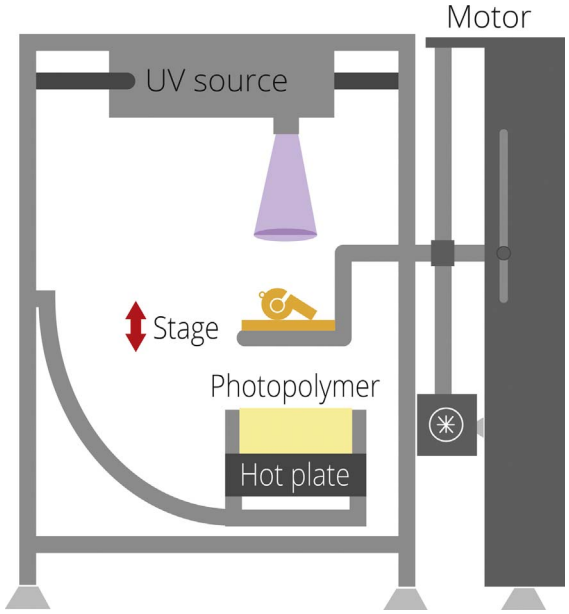

Fig. 1. Scheme of the custom-made DLP printer setup. The resin was heated by a custom-made hot plate. The reservoir used was filled with a buffer material made by a bottom layer of PDMS (approximately 1/3 of the total volume, 450 mL) covered by a thin layer of Fluorolink® (Solvay Specialty Polymers, Italy). The aim was to minimize the quantity of polymer necessary during the printing process.

2.4.2. Thermal characterization

The degree of crystallinity, χ and the melting temperature, T_m of the neat and methacrylated PCLs were evaluated with a Mettler-Toledo DSC/823e calorimeter. The samples were heated from −50 to 250 °C; the first heating rate was 10 K min^{-1}, followed by a cooling rate at 5 K min^{-1} and a second heating rate at 10 K min^{-1}. In detail, χ was calculated considering the endothermal peak of the second heating scan, considering a melting enthalpy of a 100% crystalline PCL of 134.9 J g^{-1} [48].

2.4.3. Degree of methacrylation

The methacrylation degree (D_M) was determined by ^{1}H NMR spectroscopy on a Bruker 400 MHz spectrometer using $CDCl_3$ as solvent (Fig. S1). In particular, D_M was determined according to the procedure described by Zarek et al. [31].

2.4.4. Polymer network characterization

Gel content (G%) was used to assess the degree of crosslinking of the photo-crosslinked polymers. In particular, the specimens with initial mass m_0 were placed in $CHCl_3$ (70 ml per 0.25 g of material) at room temperature under magnetic stirring for 24 h. The gel content was determined considering the mass of extracted polymer (m_e) according to the following equation:

$$G\% = 100 \cdot \left(\frac{1 - m_e}{m_0} \right) \quad (1)$$

To determine the crosslinking density, ν of the photo-crosslinked samples, dynamic-mechanical analyses (DMA) were performed in shear configuration using a Mettler Toledo DMA/SDTA861 instrument in dynamic scans from −50 to 160 °C at 3 K min^{-1} heating rate. The frequency was kept constant (1 Hz). ν was determined considering the conservative shear modulus G' at a temperature higher than the inflection point corresponding to the melting temperature T_m of the switching domains [49] (*i.e.* 90 °C) as follows:

$$\nu = \frac{G'}{RT} \quad (2)$$

where R is 8.314472 MPa cm^3 K^{-1} mol^{-1}.

2.4.5. Mechanical and shape memory effect characterization

Tensile properties for cast and printed samples were determined at room temperature by means of a Zwick/Roell Z010 (Zwick Roell, Germany) equipped with a 10 kN load cell and a longstroke extensometer, following the standard test method ASTM D638-10 (Type IV specimen, dimensions down-scaled to 44%) for the cast samples. For the printed samples, we used rectangular specimens (dimensions 62 × 6 × 3 mm) Specimens were stretched with a displacement rate of 3 and 30 mm min^{-1}. These two values of rate were selected to explore the effect of tensile test speed on mechanical properties, also taking into account the test conditions employed in previous works presenting self-healing materials [39,50]. The calculation of the elastic modulus was performed by following the same standard test method. Shape memory effect was evaluated by a custom-made equipment according to the protocol described by Lendlein et al. [28].

2.4.6. Self-healing properties

For surface damage healing analysis, an optical microscope (Olympus BX 60 with an Olympus Infinity 2 camera and a 5X objective) was employed to observe the self-healing process of cast and printed samples at the sub-macroscopic scale. A scratch was performed on specimen surfaces by using a razor blade and the samples were observed under the microscope before and after healing treatment carried out at 80 °C for 1 h. For macroscopic healing, rectangular specimens were cut into halves using blades. The two separate halves were kept separated for less than 5 min and then brought and kept in contact during the healing process (80 °C for 1 h in air). For mechanical healing, rectangular specimens were partially cut at the centre of the gauge length (Fig. S2, Supplementary Materials). Also in this case, the samples were repaired with the same healing process. Tensile tests were then performed as described in the previous paragraph. The healing efficiency η was calculated as the ratio between the maximum tensile strength of the healed sample and the maximum tensile strength of the uncut sample [40].

3. Results and discussion

The shape memory behavior was provided by PCL chains with a molecular weight of 10,000 g mol^{-1}. PCL is widely used in medical devices such as stents and biomedical scaffolds due to its biocompatible nature. It is a semi-crystalline polymer, soluble in chloroform and having a melting point ranging between 56 and 65 °C. In this work, PCL has a T_m of 56.7 °C and a degree of crystallinity of 47%, as determined by differential scanning calorimetry (DSC). In order to obtain a photocurable system with a final cross-linked structure, PCL was end-capped with 2-IEM to obtain a bifunctional PCLDMA. As determined by NMR spectroscopy, a methacrylation degree of 74% was obtained, ensuring a gel content percentage value of 96%.

Self-healing abilities were provided by introducing 2-ureido-4[1*H*]-pyrimidinone (UPy) motifs, which enable a material, if damaged, to be repaired by means of a reversible formation of four cooperative hydrogen bonds between two UPy units [51,52]. UPy motifs were incorporated into the photocurable matrix using a methacrylate monomer bearing UPy units in the side chain (UPyMA). 4D printed samples were obtained *via* UV–vis light-induced crosslinking of PCLDMA with UPyMA by a digital light projector (DLP) printer (TOP DLP Wasp, Italy). The chemical scheme of UPyMA monomer, PCLDMA and of the crosslinking reaction is shown in Fig. S3 (Supplementary Materials).

The optimal composition of the liquid blend precursor was obtained by dissolving PCLDMA and UPyMA (4 wt% with respect to the weight of PCLDMA) in $CHCl_3$ (60 wt% with respect to the total weight of UPyMA and PCLDMA) at 45 °C overnight under magnetic stirring. After adding a phosphine oxide-based photoinitiator (TPO-L, 4 wt%), the mixture was then used for the printing process. A ten-layer fashion was chosen to demonstrate the printability of the formulation. Mechanical, self-healing and shape memory properties were investigated using

Table 1
Melting temperature T_m, degree of crystallinity χ, gel content G%, crosslinking density ν and elastic modulus E for cast PCLDMA, printed and printed & repaired PCLDMA-UPyMA samples.

	T_m (°C)	χ[a] (%)	Gel content (G%)[b]	ν (mol cm^{-3})[c]	E (MPa)
Cast PCLDMA	54	37.1	95.6	$6.29 * 10^{-5}$	203 ± 50
Printed PCLDMA-UPyMA	55	29.8	81.0	$6.18 * 10^{-5}$	170 ± 38
Printed & repaired PCLDMA-UPyMA					190 ± 32

[a] Referred to $\Delta H_{100\%\ crystalline\ PCL} = 134.9\ J\ g^{-1}$.
[b] Measured by using Eq. (1).
[c] Determined by DMA analysis at 90 °C by using Eq. (2).

printed rectangular specimens. Before printing tests, the concentration of UPyMA in the liquid precursor mixture was selected by means of a parametric study to optimize shape memory effects and self-healing abilities of the final objects. PCLDMA-UPyMA samples were initially cast and photo-cured, varying the weight percentage of UPyMA between 2 and 5 wt% with respect to the weight of PCLDMA. As shown in Table S2 (Supplementary Materials), a complete recovery of permanent shape was observed for the samples with a UPyMA percentage ranging from 2 to 4 wt%. On the other hand, a 5 wt% of UPyMA hindered the full recovery of the original sample shape, due to a decrease of the degree of crystallinity passing from 29.8% with 4 wt% of UPyMA to 24.8% with 5 wt%. To assess self-repairing abilities, samples were damaged with a razor blade to produce a deep scratch and thermally treated at 80 °C for 1 h. Surface damage was repaired after this thermal treatment for all the samples (Table S2, Supplementary Materials). However, some healed scars were visible on surfaces with 2 and 3 wt% of UPyMA. For these reasons, a 4 wt% of UPyMA was found as a good trade-off between the possibility to ensure a shape memory effect and the benefit of high percentages of UPyMA on self-healing properties. This UPyMA concentration was therefore used for the following tests performed on cast and printed samples.

To better evaluate mechanical, physical and chemical properties of the new designed blend, we also prepared reference photo-cured PCLDMA samples without UPyMA by casting. As reported in Table 1, the switching temperature of the shape memory printed samples, *i.e.* T_m, is actually comparable to that of cast PCLDMA. As for the degree of crystallinity, a decrease was observed for printed PCLDMA-UPyMA samples, due to the incorporation of UPy units that likely disturbed the polymer chain crystallization and crystallites growth of PCLDMA macromolecules. The presence of UPy motifs and the printing process did not affect the crosslinking density of the samples, ν, as also confirmed by a high value of gel content. Furthermore, the introduction of UPy units appeared to have only a moderate effect on tensile properties, especially on the elastic modulus and maximum tensile strength, which are still comparable for printed PCLDMA-UPyMA and cast PCLDMA samples (Table 1 and Fig. S4, Supplementary Materials).

Cast and printed samples were further characterized in terms of mechanical properties. Fig. 2 shows the average values of maximum tensile strength and elongation at break measured at two different test speeds (3 and 30 mm min^{-1}) for cast PCLDMA, PCLDMA-UPyMA and printed PCLDMA-UPyMA. As regards the tensile strength, cast and printed samples did not exhibit any significant differences at the two values of test speeds used. Indeed, considering the values of standard deviation, no clear effect on tensile strength was observed by varying the test speeds in the range of 3–30 mm min^{-1}. Concerning the elongation at break, cast PCLDMA-UPyMA samples showed higher elongation values when compared to cast PCLDMA, likely due to the presence of four hydrogen bonded array motifs introduced by UPy groups which can enhance the ability of samples to stretch. This effect of UPy motifs on the values of elongation at break was reduced and hampered for printed PCLDMA-UPyMA, which showed an ε_B comparable to cast PCLDMA. As already shown in literature [53,54], the printing process can introduce some defects and voids between layers, thus decreasing the capability of printed materials to withstand high strains at break. This can explain why the values of ε_B measured for printed PCLDMA-UPyMA were found lower than those measured for cast PCLDMA-UPyMA.

In order to assess self-repairing abilities, which are an added value to extend the lifetime of printed objects, self-healing properties were evaluated both for surface and bulk damage. Regarding surface damage, a deep scratch was completely repaired after a thermal treatment of 1 h at 80 °C (Fig. 3a and b). As for bulk damage, a perfect binding of two parts of a specimen was demonstrated after cutting and heating with the same thermal treatment (Fig. 3c and d).

Uniaxial tensile tests were performed on mechanically damaged samples, before and after the healing cycle (see Experimental Section for details) with the aim of quantitatively evaluate self-healing properties. No significant difference of elastic modulus was found for printed PCLDMA-UPyMA specimens before and after healing (Table 1). To study the influence of UPyMA on maximum tensile strength and elongation at break of printed samples, printed PCLDMA-UPyMA were also compared to printed samples without UPyMA (Fig. 4).

The mechanical properties of printed PCLDMA were studied on rectangular bars obtained from a mixture with a 60 wt% of $CHCl_3$, which was necessary to process and print neat PCLDMA at the working temperatures of 3D printing set-up used in this work (45–50 °C). A

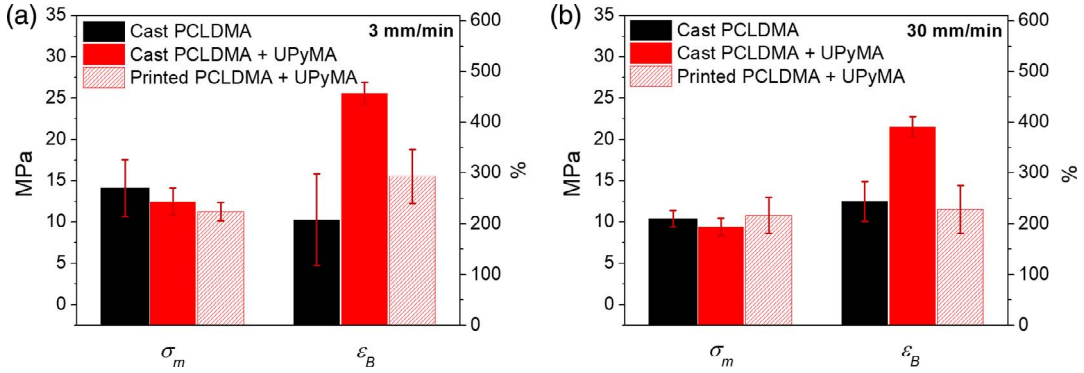

Fig. 2. Maximum tensile strength (σ_m) and elongation at break (ε_B) at T < T_m of cast PCLDMA (black), cast PCLDMA-UPyMA samples (red) and printed PCLDMA-UPyMA samples (red pattern), obtained with a tensile test speed of 3 mm min^{-1} (a) and 30 mm min^{-1} (b). (For interpretation of the references to colour in this figure legend, the reader is referred to the web version of this article.)

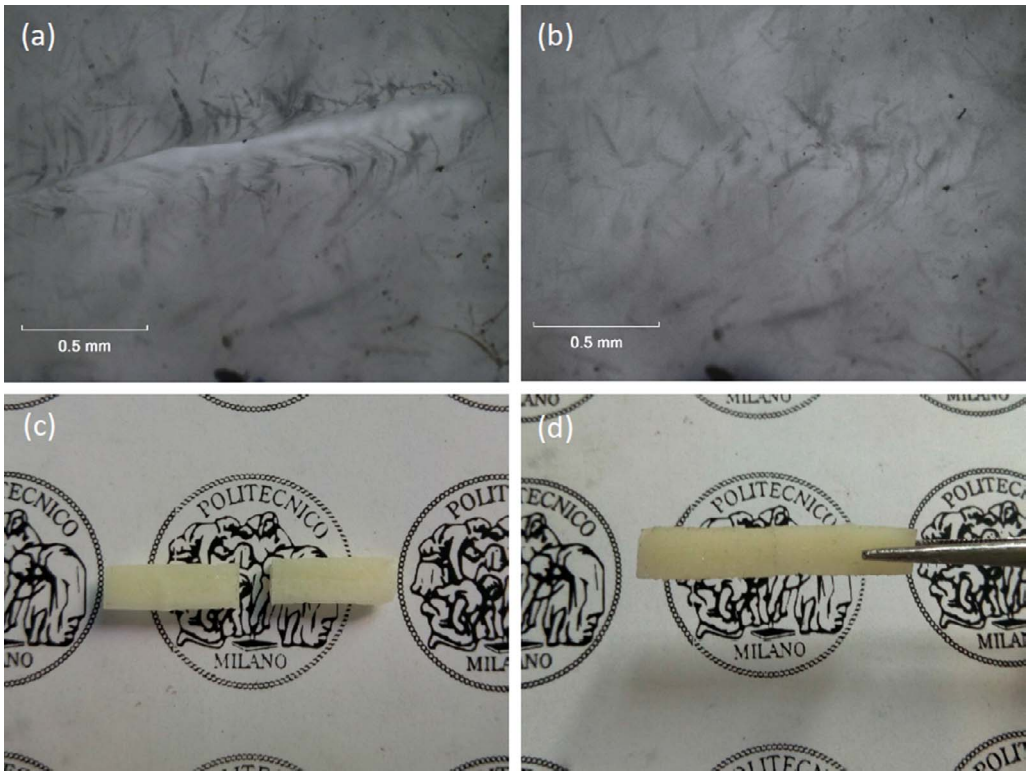

Fig. 3. Self-healing tests performed on PCLDMA-UPyMA printed samples. Images of the superficial cut before (a) and after (b) the thermal treatment at 80 °C. In addition, the knife cut in the middle of the specimen (c) is completely repaired after the same thermal treatment (d).

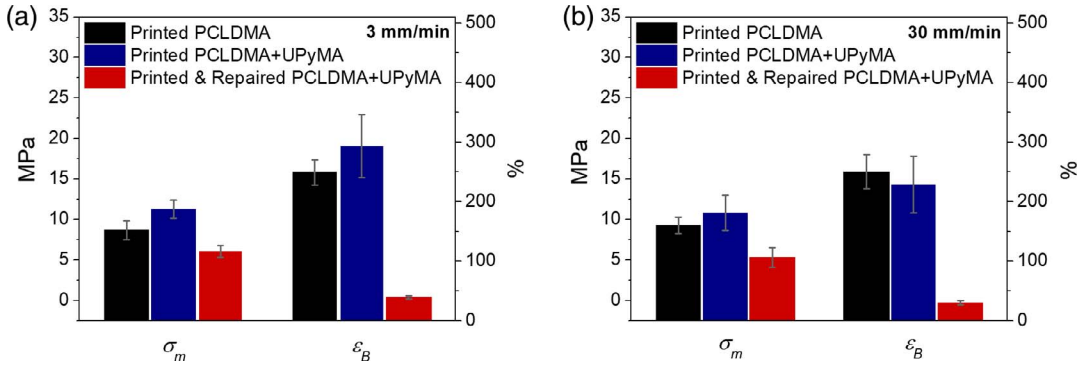

Fig. 4. Maximum tensile strength (σ_m) and elongation at break (ε_B) at T < T_m of printed PCLDMA samples (black), printed PCLDMA-UPyMA samples (blue) and self-repaired samples (red), obtained with a tensile test speed of 3 mm min^{-1} (a) and 30 mm min^{-1} (b). (For interpretation of the references to colour in this figure legend, the reader is referred to the web version of this article.)

slightly higher tensile strength was observed at an elongation rate of 3 mm min^{-1} for printed PCLDMA-UPyMA, when compared to neat printed PCLDMA. However, this difference between printed PCLDMA and PCLDMA-UPyMA appeared less evident taking into account the results obtained at 30 mm min^{-1} and the elongation at break. This demonstrates that the incorporation of UPy in the PCLDMA-based mixture does not impair mechanical performances of printed objects with the added advantage of providing self-repairing abilities. A self-healing efficiency of nearly 54% on tensile strength was calculated for printed PCLDMA-UPyMA elongated at 3 mm min^{-1}, while the recovery of the elongation performances was much lower (Table 2 and Fig. 4). Comparable healing efficiencies were obtained at varying tensile test speeds in the range of values considered for this work. Similar values of healing efficiency ranging from 50% to 80% were found for polymeric systems bearing UPy motifs by increasing the healing time, the waiting time before healing [50] and the temperature of healing [39]. The dependence of healing efficiencies upon the healing and waiting time was also observed for supramolecular rubbers from functionalized fatty acids, which are mendable via hydrogen bonds [55,56]. This suggests the possibility to further increase the healing efficiency of PCLDMA-UPyMA fabricated objects, carrying out additional studies regarding the influence of waiting and healing times on these polymeric systems in the future. Moreover, a decrease in the elongation at break for repaired samples was noticed for shorter healing times by Cordier and co-

Table 2
Healing efficiency, η (%) for cast and printed PCLDMA-UPyMA samples.

PCLDMA-UPyMA	η (%)
Cast bars 3 mm min^{-1}	41.4 ± 3.7
Cast bars 30 mm min^{-1}	40.3 ± 4.8
Printed bars 3 mm min^{-1}	53.6 ± 6.4
Printed bars 30 mm min^{-1}	51.7 ± 11.7

workers. This can explain why the elongation at break is lower for printed and repaired objects, suggesting a method for improving results. However, mechanical properties of printed PCLDMA-UPyMA samples, repaired following the procedure detailed in the Experimental Section are still adequate for applications as soft actuators [57,58]. Table 2 also shows that printed bars have a healing efficiency higher than cast samples. Considering that printed and repaired samples after tensile tests had rougher interfaces at the breaking point when compared to cast bars (Fig. S7), higher healing efficiency of printed objects can be accounted for a more efficient interpenetration between PCLDMA matrix and UPyMA and more numerous bridges between UPy groups at the razor-cut interfaces.

To evaluate the shape memory behavior, the following parameters are considered: (i) the recovery ratio R_r, which describes to which extent the polymer memorizes its original shape and (ii) the fixity ratio R_f, which defines the capability of the polymer to maintain the temporary shape. For the printed PCLDMA-UPyMA samples, R_f was 99.8% and R_r was 98.6%, demonstrating a very good reproducibility of the shape memory effect. These results also show the remarkable performances of the newly prepared smart material which exhibits shape memory properties better than other 3D printed samples [31].

Nowadays, the application of smart materials in soft robotics is fast spreading, also due to the variety of stimuli that can be used to activate both shape memory [59] and self-healing polymers [60,61]. To explore the possibility of using PCLDMA-UPyMA as support material for robotic arms and hands, we printed an "L" shaped object to mimic the index finger and the thumb. This sample was partially cut and then repaired (Fig. 5a and b).

By heating at $T > T_m$, the specimen becomes flexible and semi-transparent (due to the melting of the crystalline PCLDMA phase, also called switching segments for shape memory behavior) and can be deformed into a desired temporary shape (Fig. 5c). Once deformed, the structure is cooled down at $T < T_m$ to fix the temporary shape by the crystallization of PCL crystalline domains. At room temperature, the object is rigid and opaque. Re-heating the structure at $T > T_m$ leads to the recovery of the initial "L" printed shape, due to the melting of the crystalline phase and to the entropic elasticity (Fig. 5d–f; Movie S1 and S2). Printed and repaired samples showed shape memory properties as good as undamaged printed objects (Fig. S5, Supplementary Materials).

Supplementary Movie S1.

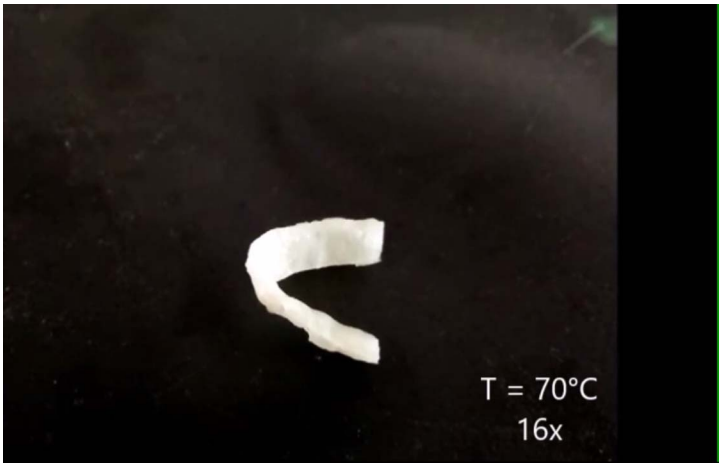

Supplementary Movie S2.

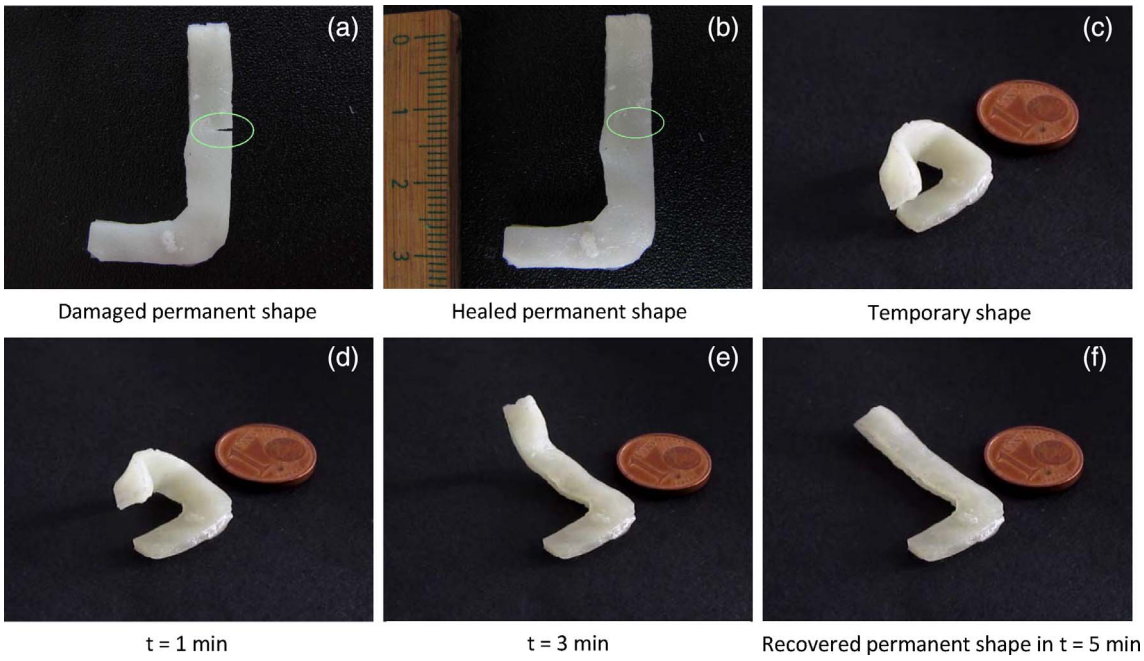

Fig. 5. Shape memory effect of PCLDMA-UPyMA repaired samples. The specimen was cut (a) and repaired after a thermal treatment of 1 h at 80 °C (b). The deformed object (c) was heated at 70 °C to start and complete the recovery of the original shape (d–f).

4. Conclusions

In summary, we have developed a novel 4D-printable smart material, which is a thermally activated shape memory polymer with self-repairing abilities, provided by self-assembling UPy units forming multiple hydrogen-bonded supramolecular structures. Our innovative approach relies on the 4D printing of this multifunctional material with a dynamic behavior by using a low-cost DLP printer. Printed objects show good self-healing behavior and remarkable shape memory properties, even after healing procedure. Mechanical properties of printed polymers are also found similar to those of neat PCL-based cast samples. In addition to this, the printed and repaired samples exhibit a healing efficiency in terms of tensile maximum stress high enough to allow their use as actuator devices in soft robotics applications, e.g. wearable devices for human-machine interaction and rehabilitation.

Acknowledgements

M.I. and R.S. contributed equally to this work. We would like to thank Mr. Stefano Cagninelli for the help to modify the 3D printer configuration adapting it to our needs.

This research did not receive any specific grant from funding agencies in the public, commercial, or not-for-profit sectors.

Appendix A. Supplementary material

Supplementary data associated with this article can be found, in the online version, at https://doi.org/10.1016/j.eurpolymj.2018.02.023.

References

[1] I. Gibson, D.W. Rosen, B. Stucker, Additive Manufacturing Technologies, Springer, New York, 2010.
[2] S.C. Ligon, R. Liska, J. Stampfl, M. Gurr, R. Mülhaupt, Polymers for 3D printing and customized additive manufacturing, Chem. Rev. 117 (15) (2017) 10212–10290.
[3] R.D. Farahani, M. Dubé, D. Therriault, Three-dimensional printing of multifunctional nanocomposites: manufacturing techniques and applications, Adv. Mater. 28 (28) (2016) 5794–5821.
[4] M. Invernizzi, G. Natale, M. Levi, S. Turri, G. Griffini, UV-assisted 3D printing of glass and carbon fiber-reinforced dual-cure polymer composites, Materials 9 (7) (2016) 583.
[5] X. Mu, T. Bertron, C. Dunn, H. Qiao, J. Wu, Z. Zhao, C. Saldana, H.J. Qi, Porous polymeric materials by 3D printing of photocurable resin, Mater. Horiz. 4 (3) (2017) 442–449.
[6] J.T. Muth, D.M. Vogt, R.L. Truby, Y. Mengüç, D.B. Kolesky, R.J. Wood, J.A. Lewis, Embedded 3D printing of strain sensors within highly stretchable elastomers, Adv. Mater. 26 (36) (2014) 6307–6312.
[7] Z. Lei, Q. Wang, P. Wu, A multifunctional skin-like sensor based on a 3D printed thermo-responsive hydrogel, Mater. Horiz. 4 (4) (2017) 694–700.
[8] S. Miao, N. Castro, M. Nowicki, L. Xia, H. Cui, X. Zhou, W. Zhu, S.-J. Lee, K. Sarkar, G. Vozzi, Y. Tabata, J. Fisher, L.G. Zhang, 4D printing of polymeric materials for tissue and organ regeneration, Mater. Today (2017).
[9] S. Tibbits, 4D printing: multi-material shape change, Arch. Des. 84 (1) (2014) 116–121.
[10] S.A. Gladman, E.A. Matsumoto, R.G. Nuzzo, L. Mahadevan, J.A. Lewis, Biomimetic 4D printing, Nat. Mater. 15 (4) (2016) 413–418.
[11] Q. Ge, A.H. Sakhaei, H. Lee, C.K. Dunn, N.X. Fang, M.L. Dunn, Multimaterial 4D printing with tailorable shape memory polymers, Sci. Rep. 6 (2016) 31110.
[12] M. Nadgorny, Z. Xiao, C. Chen, L.A. Connal, Three-dimensional printing of ph-responsive and functional polymers on an affordable desktop printer, ACS Appl. Mater. Interfaces 8 (42) (2016) 28946–28954.
[13] S.E. Bakarich, R. Gorkin, M.i.h. Panhuis, G.M. Spinks, 4D printing with mechanically robust, thermally actuating hydrogels, Macromol. Rapid Commun. 36 (12) (2015) 1211–1217.
[14] O. Kuksenok, A.C. Balazs, Stimuli-responsive behavior of composites integrating thermo-responsive gels with photo-responsive fibers, Mater. Horiz. 3 (1) (2016) 53–62.
[15] Y. Zhou, W.M. Huang, S.F. Kang, X.L. Wu, H.B. Lu, J. Fu, H. Cui, From 3D to 4D printing: approaches and typical applications, J. Mech. Sci. Technol. 29 (10) (2015) 4281–4288.
[16] F. Momeni, S.M. Mehdi Hassani, N.X. Liu, J. Ni, A review of 4D printing, Mater. Des. 122 (Supplement C) (2017) 42–79.
[17] M.A. McEvoy, N. Correll, Materials that couple sensing, actuation, computation, and communication, Science 347 (6228) (2015).
[18] Y. Lu, A.A. Aimetti, R. Langer, Z. Gu, Bioresponsive materials, Nat. Rev. Mater. 2 (2016) 16075.
[19] M.D. Hager, P. Greil, C. Leyens, S. van der Zwaag, U.S. Schubert, Self-healing materials, Adv. Mater. 22 (47) (2010) 5424–5430.
[20] H. Chaolei, L. Jiu-an, T. Xiaojun, W. Yuechao, L. Jie, Y. Yanlei, A remotely driven and controlled micro-gripper fabricated from light-induced deformation smart material, Smart Mater. Struct. 25 (9) (2016) 095009.
[21] Y. Yang, M.W. Urban, Self-healing polymeric materials, Chem. Soc. Rev. 42 (17) (2013) 7446–7467.
[22] F. Pilate, A. Toncheva, P. Dubois, J.-M. Raquez, Shape-memory polymers for multiple applications in the materials world, Eur. Polym. J. 80 (Supplement C) (2016) 268–294.
[23] L.R. Hart, J.L. Harries, B.W. Greenland, H.M. Colquhoun, W. Hayes, Healable supramolecular polymers, Polym. Chem. 4 (18) (2013) 4860–4870.
[24] Z. Wei, J.H. Yang, J. Zhou, F. Xu, M. Zrinyi, P.H. Dussault, Y. Osada, Y.M. Chen, Self-healing gels based on constitutional dynamic chemistry and their potential applications, Chem. Soc. Rev. 43 (23) (2014) 8114–8131.
[25] X.K.D. Hillewaere, F.E. Du Prez, Fifteen chemistries for autonomous external self-

healing polymers and composites, Prog. Polym. Sci. 49-50 (Supplement C) (2015) 121–153.
[26] S. Bauer, S. Bauer-Gogonea, I. Graz, M. Kaltenbrunner, C. Keplinger, R. Schwödiauer, 25th anniversary article: a soft future: from robots and sensor skin to energy harvesters, Adv. Mater. 26 (1) (2014) 149–162.
[27] C.B. Highley, C.B. Rodell, J.A. Burdick, Direct 3D printing of shear-thinning hydrogels into self-healing hydrogels, Adv. Mater. 27 (34) (2015) 5075–5079.
[28] A. Lendlein, S. Kelch, Shape-memory polymers, Angew. Chem. Int. Ed. 41 (12) (2002) 2034–2057.
[29] C.M. Yakacki, R. Shandas, C. Lanning, B. Rech, A. Eckstein, K. Gall, Unconstrained recovery characterization of shape-memory polymer networks for cardiovascular applications, Biomaterials 28 (14) (2007) 2255–2263.
[30] F.S. Senatov, M.Y. Zadorozhnyy, K.V. Niaza, V.V. Medvedev, S.D. Kaloshkin, N.Y. Anisimova, M.V. Kiselevskiy, K.-C. Yang, Shape memory effect in 3D-printed scaffolds for self-fitting implants, Eur. Polym. J. 93 (Supplement C) (2017) 222–231.
[31] M. Zarek, M. Layani, I. Cooperstein, E. Sachyani, D. Cohn, S. Magdassi, 3D printing of shape memory polymers for flexible electronic devices, Adv. Mater. 28 (22) (2016) 4449–4454.
[32] X. Li, J. Shang, Z. Wang, Intelligent materials: a review of applications in 4D printing, Assembly Autom. 37 (2) (2017) 170–185.
[33] W. Lu, X. Le, J. Zhang, Y. Huang, T. Chen, Supramolecular shape memory hydrogels: a new bridge between stimuli-responsive polymers and supramolecular chemistry, Chem. Soc. Rev. 46 (5) (2017) 1284–1294.
[34] I.V.W. Small, P. Singhal, T.S. Wilson, D.J. Maitland, Biomedical applications of thermally activated shape memory polymers, J. Mater. Chem. 20 (17) (2010) 3356–3366.
[35] M.C. Serrano, L. Carbajal, G.A. Ameer, Novel biodegradable shape-memory elastomers with drug-releasing capabilities, Adv. Mater. 23 (19) (2011) 2211–2215.
[36] M.D. Hager, S. Bode, C. Weber, U.S. Schubert, Shape memory polymers: past, present and future developments, Prog. Polym. Sci. 49 (2015) 3–33.
[37] M. Zarek, N. Mansour, S. Shapira, D. Cohn, 4D printing of shape memory-based personalized endoluminal medical devices, Macromol. Rapid Commun. 38 (2) (2017) 1600628.
[38] Y.Y.C. Choong, S. Maleksaeedi, H. Eng, J. Wei, P.-C. Su, 4D printing of high performance shape memory polymer using stereolithography, Mater. Des. 126 (Supplement C) (2017) 219–225.
[39] Y. Wu, L. Wang, X. Zhao, S. Hou, B. Guo, P.X. Ma, Self-healing supramolecular bioelastomers with shape memory property as a multifunctional platform for biomedical applications via modular assembly, Biomaterials 104 (2016) 18–31.
[40] M. Wei, M. Zhan, D. Yu, H. Xie, M. He, K. Yang, Y. Wang, Novel Poly(tetramethylene ether)glycol and Poly(ε-caprolactone) based dynamic network via quadruple hydrogen bonding with triple-shape effect and self-healing capacity, ACS Appl. Mater. Interfaces 7 (4) (2015) 2585–2596.
[41] E.D. Rodriguez, X. Luo, P.T. Mather, Linear/network poly(ε-caprolactone) blends exhibiting shape memory assisted self-healing (SMASH), ACS Appl. Mater. Interfaces 3 (2) (2011) 152–161.
[42] Y.-L. Liu, T.-W. Chuo, Self-healing polymers based on thermally reversible Diels-Alder chemistry, Polym. Chem. 4 (7) (2013) 2194–2205.
[43] K. Urdl, A. Kandelbauer, W. Kern, U. Müller, M. Thebault, E. Zikulnig-Rusch, Self-healing of densely crosslinked thermoset polymers—a critical review, Prog. Org. Coat. 104 (2017) 232–249.
[44] W. Chen, Y. Zhou, Y. Li, J. Sun, X. Pan, Q. Yu, N. Zhou, Z. Zhang, X. Zhu, Shape-memory and self-healing polyurethanes based on cyclic poly(?-caprolactone), Polym. Chem. 7 (44) (2016) 6789–6797.
[45] A. Phadke, C. Zhang, B. Arman, C.-C. Hsu, R.A. Mashelkar, A.K. Lele, M.J. Tauber, G. Arya, S. Varghese, Rapid self-healing hydrogels, Proc. Natl. Acad. Sci. 109 (12) (2012) 4383–4388.
[46] D.J.M. van Beek, A.J.H. Spiering, G.W.M. Peters, K. te Nijenhuis, R.P. Sijbesma, Unidirectional dimerization and stacking of ureidopyrimidinone end groups in polycaprolactone supramolecular polymers, Macromolecules 40 (23) (2007) 8464–8475.
[47] P. Shokrollahi, H. Mirzadeh, W.T.S. Huck, O.A. Scherman, Effect of self-complementary motifs on phase compatibility and material properties in blends of supramolecular polymers, Polymer 51 (26) (2010) 6303–6312.
[48] M. Messori, M. Degli Esposti, K. Paderni, S. Pandini, S. Passera, T. Riccò, M. Toselli, Chemical and thermomechanical tailoring of the shape memory effect in poly(ε-caprolactone)-based systems, J. Mater. Sci. 48 (1) (2013) 424–440.
[49] W. Wagermaier, K. Kratz, M. Heuchel, A. Lendlein, Characterization methods for shape-memory polymers, in: A. Lendlein (Ed.), Shape-Memory Polymers, Springer, Berlin Heidelberg, 2010, pp. 97–145.
[50] G.M.L. van Gemert, J.W. Peeters, S.H.M. Söntjens, H.M. Janssen, A.W. Bosman, Self-healing supramolecular polymers in action, Macromol. Chem. Phys. 213 (2) (2012) 234–242.
[51] L. Voorhaar, R. Hoogenboom, Supramolecular polymer networks: hydrogels and bulk materials, Chem. Soc. Rev. 45 (14) (2016) 4013–4031.
[52] R.P. Sijbesma, F.H. Beijer, L. Brunsveld, B.J.B. Folmer, J.H.K.K. Hirschberg, R.F.M. Lange, J.K.L. Lowe, E.W. Meijer, Reversible polymers formed from self-complementary monomers using quadruple hydrogen bonding, Science 278 (5343) (1997) 1601–1604.
[53] A.R. Torrado, D.A. Roberson, Failure analysis and anisotropy evaluation of 3D-printed tensile test specimens of different geometries and print raster patterns, J Fail. Anal. Preven. 16 (1) (2016) 154–164.
[54] A.R. Torrado Perez, D.A. Roberson, R.B. Wicker, Fracture surface analysis of 3D-printed tensile specimens of novel ABS-based materials, J. Fail. Anal. Preven. 14 (3) (2014) 343–353.
[55] P. Cordier, F. Tournilhac, C. Soulié-Ziakovic, L. Leibler, Self-healing and thermoreversible rubber from supramolecular assembly, Nature 451 (2008) 977.
[56] D. Montarnal, P. Cordier, C. Soulié-Ziakovic, F. Tournilhac, L. Leibler, Synthesis of self-healing supramolecular rubbers from fatty acid derivatives, diethylene triamine, and urea, J. Polym. Sci., Part A: Polym. Chem. 46 (24) (2008) 7925–7936.
[57] B.C.K. Tee, C. Wang, R. Allen, Z. Bao, An electrically and mechanically self-healing composite with pressure- and flexion-sensitive properties for electronic skin applications, Nat. Nano 7 (12) (2012) 825–832.
[58] R.V. Martinez, A.C. Glavan, C. Keplinger, A.I. Oyetibo, G.M. Whitesides, Soft actuators and robots that are resistant to mechanical damage, Adv. Funct. Mater. 24 (20) (2014) 3003–3010.
[59] C. Lee, M. Kim, Y.J. Kim, N. Hong, S. Ryu, H.J. Kim, S. Kim, Soft robot review, Int. J. Control Autom. 15 (1) (2017) 3–15.
[60] T.-P. Huynh, P. Sonar, H. Haick, Advanced materials for use in soft self-healing devices, Adv. Mater. 29 (19) (2017) 1604973.
[61] L. Hines, K. Petersen, G.Z. Lum, M. Sitti, Soft actuators for small-scale robotics, Adv. Mater. 29 (13) (2017) 1603483.